Dynamic digestion of a high protein beverage based on amaranth: Structural changes and antihypertensive activity

Santiago E Suárez, Hanitra Rabesona, Olivia Ménard, Julien Jardin, Marc Anton, María Cristina Añón

Food Research International 187 (2024) 114416

Contents lists available at ScienceDirect

Food Research International

journal homepage: www.elsevier.com/locate/foodres

Dynamic digestion of a high protein beverage based on amaranth: Structural changes and antihypertensive activity

Santiago E. Suárez [a,b,c], Hanitra Rabesona [b], Olivia Ménard [c], Julien Jardin [c], Marc Anton [b], María Cristina Añón [a,*]

[a] Centro de Investigación y Desarrollo en Criotecnología de Alimentos (CIDCA), Facultad de Ciencias Exactas, UNLP. CIC. CONICET (Consejo Nacional de Investigaciones Científica y Técnicas), Calle 47 y 116 – 1900, La Plata, Argentina
[b] INRAE, UR BIA, F-44316 Nantes, France
[c] INRAE, Institut AGRO, STLO, 35042 Rennes, France

ARTICLE INFO

Keywords:
Amaranth beverage
Amaranth antihypertensive peptides
Dynamic *in vitro* digestion

ABSTRACT

An amaranth beverage (AB) was subjected to a simulated process of dynamic gastrointestinal digestion DIDGI®, a simple two-compartment *in vitro* dynamic gastrointestinal digestion system. The structural changes caused to the proteins during digestion and the digesta inhibitory capacity of the angiotensin converting enzyme (ACE) were investigated. In gastric compartment the degree of hydrolysis (DH) was 14.7 ± 1.5 % and in the intestinal compartment, proteins were digests in a greater extent (DH = 60.6 ± 8.4 %). Protein aggregation was detected during the gastric phase. The final digesta obtained both at the gastric and intestinal level, showed ACE inhibitory capacity (IC_{50} 80 ± 10 and 140 ± 20 μg/mL, respectively). Purified fractions from these digesta showed even greater inhibitory capacity, being eluted 2 (E2) the most active fraction (IC_{50} 60 ± 10 μg/mL). Twenty-six peptide sequences were identified. Six of them, with potential antihypertensive capacity, belong to *A. hypochondriacus*, 3 agglutinins and 3 encrypted sequences in the 11S globulin. Results obtained provide new and useful information on peptides released from the digestion of an amaranth based beverage and its ACE bioactivity.

1. Introduction

Consumption habits are changing while world population continues to increase. Transition to more sustainable and healthier diets mainly based in plant-based products is a reality in population who can afford the cost of these products. In this way, non-dairy plant-based beverages are installed as a good alternative to incorporate new vegetable healthy nutrients because of the presence of bioactive components with health-promoting properties, which attract health-conscious consumers (Munekata et al., 2020). Nutritional reasons such as milk protein allergies, lactose intolerance, absence of saturated fats, as well as environmental concern and habits changes in food consumption increase the interest in these products (Craig & Fresán, 2021). Protein content is an important factor of plant-based beverages as a substitute of dairy milk as consumers desire the protein level to approach the level of cow's milk. The most common sources for plant-based beverages include cereals, legumes, nuts, seeds, and pseudocereal-based (Munekata et al., 2020). As an emerging protein source, the grain of amaranth has taken more relevance. Indeed, this culture well known as an ancestral crop native to the Mesoamerica contains an excellent aminoacidic balance, rich in lysine (4.6–6.1 g/100 g protein), a limiting amino acid in cereals, while protein content varies from 13.0 % to 18.4 % on dry weight basis depending on the species (Velarde-Salcedo et al., 2019). A high protein beverage was developed in our laboratory through alkaline solubilization of proteins, starch removal by centrifugation and colloidal stabilization by gum mixture addition (Manassero et al., 2020). As was showed in this study, it was possible to formulate a nutritionally good amaranth beverage (AB) with appropriate stability characteristics. Protein content was 3.42 g/100 g sample, equivalent to cow's milk and calcium content was 14.48 mg/100 g sample, higher than other plant-based drinks (Munekata et al., 2020).

Futhermore, numerous studies have shown that amaranth grain, particularly proteins and encrypted peptides have a protective effect on cardiovascular system (Añón et al., 2021).

Antihypertensive peptides derived from amaranth proteins were extensively studied (Nardo et al., 2020). Inhibition against the enzymes

* Corresponding author.
E-mail address: mca@biol.unlp.edu.ar (M. Cristina Añón).

https://doi.org/10.1016/j.foodres.2024.114416
Received 2 November 2023; Received in revised form 20 April 2024; Accepted 22 April 2024
Available online 24 April 2024

who participate in RAAS system (Renin-Angiotensin-Aldosterone System), one of the main regulators of blood pressure in human body, such as angiotensin converting enzyme and renin, was reported (Ayala-Niño et al., 2019; Fritz et al., 2011; Quiroga et al., 2012, 2017; Suárez et al., 2020). These peptides could be releasing from the parent protein for different techniques: fermentation, enzyme hydrolysis using microbial proteases or sequential action of pepsin and pancreatin, main enzymes of gastrointestinal digestion. *In vitro* gastrointestinal digestion has gained in the last years more relevance due to a more realistic approach. Many systems have been developed as well as many protocols have been used. In the past years, consensus protocol INFOGEST, for protein foods and static digestion, has taken more relevance and agreement in the scientific community. In the present work, to better understand the biological benefit of this product, amaranth beverage was subject to a gastrointestinal digestion using a dynamic system. Dynamic systems are closer to physiological conditions and are more promising to accurately mimic the digestive process (Dupont et al., 2019). The DIDGI® model, was built to monitor the disintegration and the kinetics of hydrolysis of the food occurring during a simulated digestion. Gastric and intestinal transit times, the kinetics of pH, digestive secretions and stirring are controlled by a computer system to be physiological realistic (Ménard et al. 2015). Precisely, a DIDGI® system was utilized to reproduce gastric and duodenal digestions, and then assess the structural changes in proteins during these phases. To date, no studies have used a dynamic *in vitro* digestion system to describe the behavior of amaranth protein. The aim of this work was to study the structural changes of amaranth proteins during gastrointestinal digestion using a DIDGI® system and evaluate angiotensin converting enzyme inhibition to identify potential bioactive peptide sequences. To our knowledge, this is the first time that the structural changes suffered by the proteins present in an amaranth beverage during the simulation of the dynamic gastrointestinal process and the antihypertensive peptides generated during the process have been analyzed.

2. Materials and methods

2.1. Chemicals and reagents

Porcine pepsin (P6887; 3672 U/mg), porcine pancreatin (P7545; 75 U/mg), bovine bile extract (B3883) and the enzyme inhibitors pepstatin A (P5318) and Pefabloc (76,307) were all obtained from Sigma-Aldrich (St. Quentin Fallavier, France). All chemicals used for the simulated fluids were purchased from Sigma Aldrich.

2.2. Preparation of amaranth beverage

Amaranth slurries were prepared following the procedure described by Manassero et al. (2020). Briefly, Amaranth seeds (*Amaranthus hypochondriacus* var. antorcha), harvested in Rio Cuarto, Córdoba, Argentina, were ground using a colloidal mill (model AD 35-R, ColMil, Argentina) during 1 min at 20 °C with gellan gum (GG), and xanthan gum (XG), dispersions in Milli-Q water. Water: seeds proportions were 1:3 and the concentration of GG and XG was 0.015 g and 0.020 g/100 g of dispersion, respectively. After grinding, pH was adjusted to 10 and kept under magnetic stirring for 2 h at 25 °C. Then, samples were centrifuged at 6000 g for 20 min at 20 °C (Beckman Coulter Avanti J-25 (Brea, California, USA)), the supernatant was filtered, and the pH was adjusted to 7.3. Finally, beverages were heated 20 min at 85 °C, cooled and frozen at −80 °C prior being to freeze dried. Amaranth beverage powder (ABP) was kept at −4°C until use. Amaranth beverage composition was 3.75 ± 0.03 of proteins, 0.55 ± 0.02 for lipids, 1.08 ± 0.02 for fiber, 0.62 ± 0.06 for ashes, 3.07 for carbohydrates and 90.3 ± 0.7 water, g/100 mL sample.

2.3. Dynamic digestion DIDGI® system

ABP was rehydrated in Milli-Q water at 10 % w/v with magnetic agitation and kept at 37 °C before digestion. The pH of the fresh amaranth beverage (AB) was 7.4. Dynamic *in vitro* digestion was performed in a DIDGI® system (Ménard et al., 2014). Two consecutive compartments were used simulating the stomach and duodenal conditions. Gastrointestinal conditions were chosen to simulate adult digestions conditions and were selected based on literature data (Egger et al., 2019), parameters are summarized in Table 1. The pepsin amount was based on the activity of the powder and fixed to cover 2000 units/mL of gastric content. The intestinal conditions were set up as reported by (Minekus et al., 1995). Oral phase was omitted due to the study of a liquid beverage. Gastrointestinal digestion of AB was performed in triplicate. Samples were taken at 0, 15, 30, 60, 90 and 105 min of gastric digestion and after 15, 30, 60, 90, 120, 150 and 180 min of intestinal digestion. Final digesta was obtained after dynamic digestion finished at 180 min. Samples were frozen after the addition of Pepstatin A (1 μM) for pepsin inhibition and Pefabloc® (5 mM) for intestinal digesta inhibition as final concentration.

2.4. Particle size distribution

Particle size distribution was determined in gastric digesta by light scattering (Malvern Mastersizer 2000, Worcestershire, UK). The scattering of particles was accurately predicted by the Mie scattering model. The refractive index (RI) of dispersed protein particles was 1.52 and the RI for water was 1.33. Amaranth beverage (t = 0) and gastric digesta were dispersed in water in the stirred dispersion unit and the measure was done when obscuration reached around 10 %. Protein particle size is reported as the mean volume–based diameter or De Broucker diameter ($D_{4,3}$). Aggregation index (AI) was calculated as Equation (1) previously reported by (Suarez & Añón, 2017). Volumes of initial and gastric samples were also measured and dispersed in 2 % (w/v) SDS solution (1:1, v/v) and gently mixed for a few seconds before the particle size measurement.

Table 1
Gastrointestinal conditions for the *in vitro* dynamic digestion of amaranth beverage simulating adult conditions. SGF (simulated gastric fluid) and SIF (simulated intestinal fluid).

Gastric conditions (37 °C)		
SGF (Simulated Gastric Fluid)	Na^+	100 mM
Stock solution at pH 6.5	Ca^{+2}	1 mM
	K^+	13 mM
Fasted volume	SGF	24 mL
Amaranth Milk	Ingested amount	100 mL
Fasted Gastric pH	pH	2.2
pH acidification curve	pH	$pH = 1.68 + 4.32^{(-t/65)}$
	Pepsin	
	Flow rate	1 mL/min from 0 to 10 min
	Flow rate	0.5 mL/min from 10 min to end
Gastric emptying (Elashoff fitting)	$t_{1/2}$	35 min
	β	1.15
Intestinal conditions (37° C)		
SIF (Simulated Intestinal Fluid)	Na^+	100 mM
Stock solution at pH 6.5	Ca^{+2}	1 mM
	K+	13 mM
Intestinal pH	pH	6.5
Secretion	Bile	4 % from 0 to 30 min
	Bile	2 % from 30 to the end
	Flow rate	0.5 mL/min from 0 to the end
	Pancreatin	7.0 %
		0.25 mL/min from 0 to the end
Intestinal emptying	$t_{1/2}$	85 min
	β	1.4

$$AI = \left(D_{4,3t} - D_{4,3t+SDS}\right)/D_{4,3t+SDS} \quad (1)$$

2.5. Gel electrophoresis

Protein composition was characterized by SDS-PAGE with Mini-Protean TGX Precast Gradient Gels 4–20 % using Mini-Protean Tetra Cell system (Bio-Rad Life Science, France). All reagents were from Bio-Rad Life Science. Samples of AB taken from the gastric and intestinal compartments during DIDGI® were diluted in 2x Laemmli sample buffer in reducing conditions with 2-mercaptoethanol 5 % w/v and then heated at 100 °C for 5 min. Ten μL of each sample were loaded on the well (20 μg of protein/well). The migration buffer contained 25 mM Tris, 192 mM glycine, 0.1 % SDS according to (Laemmli, 1970) protocol. Molecular weight (MW) protein marker from MW 14.4 to 116 kDa (unstained Molecular weight marker, Euromedex, Souffelweyersheim, France) was used for calibration. The migration was carried out at 150 V for 45 min. The gel was stained with a solution of Coomassie Brilliant Blue G-250 for 2 h with agitation according to (Lawrence & Besir, 2009). The gel was rinsed with distilled water before scanning on a flatbed scanner (Image Scanner iii; GE Healthcare, Souffelweyersheim, France).

2.6. Degree of hydrolysis (DH)

The degree of hydrolysis was calculated by determination of free amines released during gastrointestinal digestion. Samples were centrifuged for 20 min at 10.000 g and at 4 °C and the supernatants were used. The assay was performed by reacting the digested sample with o-phthaldialdehyde (OPA) and β-mercaptoethanol according to Bertrand-Harb et al. (1993). The absorbance was measured at 304 nm. Leucine was used for measurement of the standard curve (0 to 2,5 mM). The degree of hydrolysis was calculated according to Equation (2), after considering the sample dilution by secretions and the gastro-intestinal emptying.

$$DH(\%) = \frac{\left[NH_{2digesta}\right] - \left[NH_{2secretions}\right] - \left[NH_{2sample}\right]}{\left[totalNH_{2sample}\right] - \left[NH_{2sample}\right]} x100 \quad (2)$$

where NH_2 digesta was the concentration of primary amines after t min digestion, NH_2 sample was the concentration of primary amines in the AB before digestion, NH_2 secretions was the primary amino group content of bile and pancreatin solutions as the same concentrations as those found in intestinal digesta and total NH_2 sample was the total primary amines in the amaranth juice. All values were expressed in mg/L of NH_2.

2.7. Fractionation and RP-HPLC analysis

Fractionation was performed using Waters Sep-Pak cartridges Vac 20 cc C18-5 g (Waters, Saint-Quentin-en-Yvelines Cedex, France). Cartridges were conditioned and washed with 5v of column of solvent B (acetonitrile/water 98/2 (v/v) with (0.04 % TFA), followed by an equilibration step using water/acetonitrile 70/30 (v/v) with (0.0 4 % TFA) and finally solvent A (water/acetonitrile 98/2 (v/v) with trifluoracetic acid (0.05 % TFA). For fractionation, 100 mg of freeze dried final digesta was dissolved in 5 mL of Milli-Q water and then centrifuged at 10.000 g for 30 min at 20 °C (Sigma D-37520 Nr.12154-H (Harz, Germany)). Five mL of supernatant (3.8 mg protein/mL) was loaded onto the cartridge. Then, a washing step was done with solvent A and unretained (**UR**) fraction was collected. Consecutively, water/acetonitrile 70/30 (v/v) with (0.04 % TFA) and solvent B were used for sample's elution and collected eluted 1 (**E1**) and eluted 2 (**E2**), respectively. Fractions were evaporated in a Savant Speedvac SC110A concentrator (Holbrook, NY, USA) to discard acetonitrile and were used for HPLC analysis and for activity studies. Then, fractions were frozen at −80 °C and freeze dried. Analysis of the digesta and fractions was carried out on a RP-HPLC using a Dionex Ultimate 3000 system (Thermo Fisher Scientific, Courtaboeuf Cedex, France). A symmetry RP C18 column 3.5 μm, 4.6 mm x 100 mm, (Waters, Milford, MA, USA) was equilibrated with solvent A at a flow rate of 1 mL/min. Elution was carried out at 20 °C by applying solvent gradient from 0-30 % of solvent B over 22 min and finally 100 % B until 25 min. Detection of peptides was monitored by UV detection at 216 nm and 280 nm using RS variable wavelength detector (Dionex, VND3400R5). Samples were centrifuged at 10.000 g, 10 °C, 30 min before loading on the column.

2.8. ACE inhibitory activity

ACE-inhibitory activity was assayed according to (Cushman & Cheung, 1971), with some modifications (Quirós et al., 2005). Briefly, to determine the inhibition activity, 100 μL of sodium borate buffer pH 8.3 containing 0.3 M NaCl was mixed with 40 μL of digesta samples, (gastric t = 105 min, final digesta, UR, E1 and E2), 40 μL of the commercial enzyme (EC 3.4.15.1, 10 mU, 1U/mg; Sigma) and were incubated with 70 μL of synthetic substrate (HHL, 5 mM) at 37 °C for 30 min. For maximum activity control, 40 μL of milli Q water were used instead of digesta. The reaction was stopped by the addition of 0.15 mL of 1 M HCl. The hippuric acid generate was extracted with 1.5 mL of ethyl acetate, centrifuged 5 min at 5000 g and 20 °C, 1 mL of ethyl acetate carefully taken was heat-evaporated at vacuum for 30 min. The absorbance was measured at 228 nm in a microplate reader (BioteK Epoch, Highland, USA). Controls containing captopril were also performed.

2.9. LC-MS/MS analysis

Mass spectrometry (MS) analysis was conducted as described previously (Deglaire et al., 2019) with some modifications. Fraction E2 as described in the section 2.7 was analyzed by ESI-MS and MS/MS infusion then in NanoLC ESI-MS with a direct injection assembly to avoid losing material that would not remain attached to the preconcentration cartridge. Acquisitions were performed in positive mode. Experiments were performed on a Q-Exactive mass spectrometer (Thermo Scientific, San Jose, CA, United States) equipped with a nano-electrospray ion source coupled to a nano RSLC Dionex U3000 system (Thermo Scientific). One μL of sample was injected into a system NanoLC Dionex U3000 RSLC by direct injection mode. Elution at a flow rate of 300 nL/min was carried on a separation column C18 (pepMap100 reversed-phase, 3 μm particle size, 100 Å pore size; Dionex, Amsterdam, Netherlands), 75 μm inner diameter by 250 mm length, at 35 °C. The mobile phases used were solvent A (2 % acetonitrile, 0.08 % formic acid and 0.01 % trifluoroacetic acid in deionized water) and solvent B (95 % acetonitrile, 0.08 % formic acid and 0.01 % trifluoroacetic acid in deionized water). Elution gradient was applied from 5 % to 35 % (v/v) solvent B in solvent A over 40 min followed by 35 % to 85 % solvent B over 5 min, then 85 % to 3 % solvent B over 10 min and returned to 5 % solvent B over 10 min for column equilibration. The separated peptides were ionized in the Proxéon source with an optimized voltage of 2 kV. The inlet capillary of the spectrometer was heated to a temperature of 250 °C. The mass spectra were recorded at a resolution of 70,000 between m/z 200 and 2000 and the MS/MS fragmentations were carried out on the 10 most intense MS ions. After fragmentation of an ion, the MS/MS spectrum was recorded at a resolution of 17,500 and the ions of the same m/z ratio were excluded for 20 s.

2.10. Peptide identification

The raw MS files were processed by MSConvert in. mzML file (peak picking level 1–2) before interpretation using the software i2MassChroQ (version0.4.62) previously named X!Tandem pipeline software (Langella et al., 2017). The database used for peptide identification was the Amaranthus tricolor reference genome ASM2621246v1 downloaded from the National Center for Biotechnology Information (https://www.ncbi.nlm.nih.gov, NCBI RefSeq assembly GCF_026212465.1). Pepsin

being an enzyme with low specificity, performing a database search against such large proteome could provoke reaching computational limits in terms of memory usage or search time. In order to avoid this, we decided to use a two-step search strategy. In the initial step a search was carried out with fairly restrictive parameters (tryptic or semi-tryptic cuts) against the full protein database. The results obtained from this non definitive first step were validated by the software i2MassChroQ: peptides identified with an e-value < 0.01 were automatically validated and a minimum of 2 peptides was authorized to validate a protein. The proteins identified through this initial search were compiled and added to the fasta files of the taxonomy 3563 'amaranthaceae' (3924 proteins) downloaded from the uniprot website (https://uniprot.org/) as well as the **c**ommon **R**epository of **A**dventitious **P**roteins (cRAP protein sequences, https://www.thegpm.org/crap/) and *sus scrofa* proteome (for enzymes and digestion fluids) to build a "homemade database" that will then be used in the second step for final peptide identification with high confidence. The search parameters used in the second step against this "homemade database" were as follow: i) pepsin specificity being low at certain pH, we considered a nonspecific enzyme cleavage; ii) mass tolerances were set at 0.05 Da for fragment ions and 10 ppm for parent ions, iii) the potential modifications allowed were serine or threonine phosphorylation and methionine oxidation. The results obtained for peptide identification in the second step were validated by the software i2MassChroQ with a maximum peptide e-value of 0.05 and a minimum of three peptides per protein. Peptides with a minimal length of 6 amino acids were considered.

2.11. Statistical analysis

The statistical analysis was performed with the GraphPad Prism 6.0 (GraphPad Prism Inc., CA, USA). The results obtained in the experiments were expressed as means ± standard deviation of the mean (SD). *In vitro* dynamic digestion was performed in triplicate. To compare mean values, a one-way analysis of variance (ANOVA) multiple comparisons was applied. The critical significance level was set at $p < 0.05$. The Least Significant Difference (LSD) test was used to analyze the results obtained for degree of hydrolysis and particle size.

3. Results and discussions

3.1. pH variation during the gastric phase

For the simulation of the gastrointestinal digestion process, a DIDGI® system unit was used that allows the progressive addition of pepsin and HCl (to the SGF) and the gastric emptying. Fig. 1**a** shows the decrease of pH with the increase of the digestion times. During the first 5 min of the process, the pH of the gastric compartment changed from 2.92 ± 0.6 to 6.38 ± 0.44. After 15 and 30 min of digestion, the pH reached values of 5.06 ± 0.09 and 4.45 ± 0.01, respectively, and it continues to decrease, practically linearly, until 100 min of digestion, which coincides with the gastric emptying. At this time, the pH value was 2.45 ± 0.13 (Fig. 1**a and b**). The same trend was registered for the triplicates made. The pH profile obtained was similar but not equal to that reported for other food matrices such as soy protein/milk protein blended beverages, soy milk, and almond milk (Wegrzyn et al., 2021, Wang et al., 2020, 2021). It should be noted that the variation in pH reflects the buffering capacity of the sample analyzed, as has been reported for dispersions of pea and rice proteins (Jiménez-Munoz et al., 2021) and soy protein/milk protein blended beverages (Wegrzyn et al., 2021). Apparently, the proteins in the AB would have a lower buffering capacity than that corresponding to milk proteins, more similar to that corresponding to soybean and pea proteins and lower than those of rice proteins. These differences would be associated with amino acids composition of the proteins in particular aspartic and glutamic acid residues (Mennah-Govela et al., 2019). The proteins present in AB contain a high content of these two amino acids (Table 2).

3.2. Protein hydrolysis

3.2.1. Degree of hydrolysis

The protein hydrolysis was evaluated by measuring the released of primary amines (NH_2) and by sodium-dodecyl-sulfate polyacrylamide gel electrophoresis at different time point. For both methods, amaranth beverage was analyzed at various time points after the beginning of each digestive phase, as indicated in Materials and methods. Fig. 2 shows the evolution of DH during the simulated gastrointestinal digestion process. During the gastric phase, the DH was 2.1 ± 0.1 at 30 min and 5.0 ± 0.4 % at 60 min ($p < 0.001$), to later reach values of 8.2 ± 0.7 and 14.7 ± 1.5 % after 90 ($p < 0.0005$) and 105 min ($p < 0.0001$) of digestion. In the intestinal compartment, proteolysis increased, reaching values to 27.4 ± 5.4 % and 33.7 ± 2.6 % between 15 and 150 min without any

Table 2
Aminoacidic (AA) composition of Amaranth beverage (AB). Composition is expressed in mg amino acid/100 g protein.

AA (g/100 g protein)	AB
A.aspartique + Asparagine (Asx)	7.44 ± 0.2
A.glutamique + Glutamine (Glx)	16.56 ± 0.29
Serine	3,83 ± 0.06
Glycine	4.64 ± 0.08
Threonine	2.19 ± 0.06
Histidine	7.44 ± 0.19
Alanine	2.86 ± 0.09
Arginine	6.19 ± 0.10
Proline	3.56 ± 0.06
Tyrosine	1.75 ± 0,04
Valine	5.00 ± 0.08
Cysteine	0.25 ± 0.08
Methionine	1.53 ± 0.02
Isoleucine	3.69 ± 0.07
Leucine	4.92 ± 0.14
Phenylalanine	1.82 ± 0.10
Tryptophane	2.24 ± 0.12
Lysine	1.41 ± 0.17

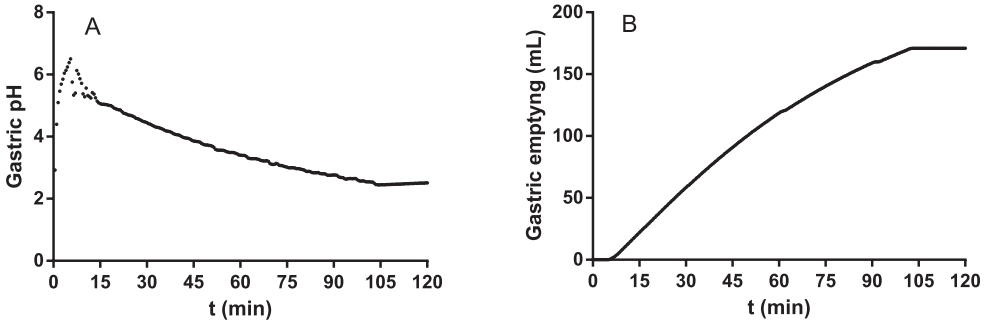

Fig. 1. Changes in pH (A) and gastric emptying (B) during dynamic gastric digestion.

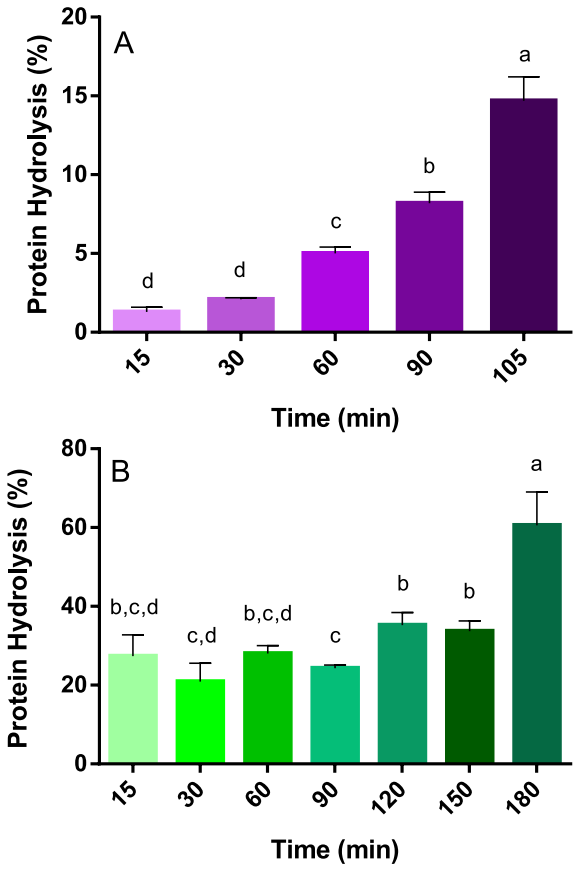

Fig. 2. Degree of protein hydrolysis (DH) in gastric (A) and intestinal (B) compartments over *in vitro* dynamic digestion of AB. Different letters means significative difference ($p < 0.05$).

significance difference. In the final time, 180 min, the DH was 60.6 ± 8.4 % ($p < 0.0001$). The increase in DH at the beginning of the intestinal phase could be attributed to the structural changes experienced by the amaranth proteins during the first minutes they remain in the stomach compartment before gastric emptying begins. These changes are related to the partial solubilization and unfolding that the AB proteins would undergo due to the pH variation (pH 2.92 ± 0.6 to 6.38 ± 0.44) previously discussed (Fig. 1**a**), which would also allow a slight hydrolytic action of pepsin. These structural amaranth protein variations have been previously studied in our laboratory (Martinez & Añón, 1996). The structural proteins modifications added to the enzyme/substrate ratio and pH of the intestinal compartment, would facilitate the hydrolytic action of trypsin. Otherwise, according to composition of amino acids performed **(**Table 2**)** the proteins present in the AB are rich in the amino acids required for the cleavage of the peptide bond by the enzymes present in the intestinal phase, which would facilitate its hydrolysis. Rodríguez & Tironi (2023) prepared an amaranth beverage from *Amaranthus manteggazianus* seeds and after an *in vitro* static digestion process found a DH of 38 ± 2 %, this value obtained by TNBS method was similar to others amaranth samples digested by an *in vitro* static method (Rodríguez & Tironi, 2020). Similar values were found during dynamic intestinal phase of AB at 120 min (35.2 ± 3.2 %) and 150 min (33.7 ± 2.6 %) but the final DH after 180 min was higher than static method, 60.6 ± 8.4 %.

3.2.2. SDS-PAGE analysis

SDS-PAGE patterns of the protein profiles of the gastrointestinal digestion under reducing conditions are shown in Fig. 3**.** The AB, before being subjected to simulated gastrointestinal digestion process, presents twelve polypeptide species (Fig. 3**, lane AB**). According to previous results obtained in our laboratory, these bands could be assigned to the albumin and globulin fractions (Martínez et al., 1997; Martínez & Añón, 1996; Quiroga et al., 2010). The first three bands of MW 56.9, 45.3, 40.1 KDa would correspond to P and 7S globulins, the two subsequent bands of 34, and 31.9 KDa to albumins and/or basic polypeptides of 11S globulin and P globulin, the triplet of 25.0, 22.5, and 20.9 to basic polypeptides of 11S globulin and P globulin and in the lower part of the gel bands of 18.2, 11.9, 9.8 and 8.6 kDa, all of them belonging to the albumin fraction. The 18.2 kDa polypeptide species could also belong to 7S globulin. The presence of species corresponding to the glutelin fraction cannot be ruled out, which presents a polypeptide profile equivalent to globulins 11S and P globulin. These results agree with the results recently obtained by Manassero et al. (2020). After 15 min of gastric digestion, the polypeptide profile was equivalent to that of AB except for the presence of high molecular mass aggregates at the top of the gel. These aggregates may have been formed by the decrease of pH in the gastric compartment from the original value of AB to 5.06 (Fig. 1), a value close to the average isoelectric point (pI) of amaranth proteins; the pI of globulin proteins is 5.0 – 4.8 with a maximum insolubility at pH 4.5–6 (Marcone & Yada, 1992; Konishi et al., 1985) and pI of albumin proteins 7–7.5 and 4.0–4.5 (Konishi et al., 1991; Segura-Nieto et al., 1992). They could also be due to the action of the acid medium and/or the partial action of pepsin on the aggregates originally present in AB, a consequence of the presence of xanthan and gellan gums and the heat treatment carried out during its formulation and production (Manassero et al., 2020). After 30 min of digestion, only the marked decrease of a 56.9 kDa band corresponding to P globulin was observed (Fig. 3**, line 30**). At 60 min of digestion, the pH of the medium reached a value of 3.3 (Fig. 1), which allowed the protonation of the polypeptide species present in the digesta, unfolding, and partial solubilization of the aggregates present. In addition, the disappearance of practically all the initial polypeptide species was detected except for those corresponding to 40.1 and 20.9 kDa and the appearance of low molecular mass peptide species from hydrolysis (Fig. 3, **line 60**). It should be noted that pepsin is more active at a pH between 2 and 4 and is permanently deactivated at a pH above 8. According to the previously discussed pH profile (Fig. 1**a**), pH 4 is reached approximately after 40 min of digestion, time from which pepsin would begin its full hydrolytic activity. The one with the lowest MW, 20.9 kDa, could correspond to the basic globulin subunit, although it cannot be ruled out that it belongs to the fraction of albumins and/or glutelins and the species of 40.1 kDa could be assigned to globulin and/or 7S globulin. At the end of gastric emptying, 105 min, (Fig. 1**b**) practically all the protein species present in AB have disappeared and low MW polypeptides, products of hydrolysis, were observed (Fig. 3**, lines 90 and 105**).

After 5 min of digestion, gastric emptying begins, so the semi-digested chyme is received in the intestinal compartment. At 15 min of digestion, the peptide profile of the intestinal compartment was very similar to that of the 15 and 30 min gastric profiles. The biggest differences reside in the appearance of polypeptide species of MW > 110 kDa, probably coming from the aggregates formed at the gastric level due to pH effects plus the non-soluble aggregates present in the original AB, which were attacked and solubilized by the action of pancreatin (Fig. 3**, lines 15 and 30**). The disappearance of some of the high MW polypeptide species, greater than 116 kDa, and a better detection of the hydrolysis products of MW < 14 kDa were also observed. After 60 min of intestinal digestion, the attenuation of the specie of 20.9 kDa was detected, which would seem to disappear after 90 min. Between 60 and 120 min two bands remains in the gel: 31.9 kDa and 25 kDa, it would correspond to basic subunit of 11S globulin and P globulin. These two polypeptides were present in the gastric phase until 30 min, they disappeared after 60 min; the presence in the intestinal phase would come from gastric emptying during the first 30 min. The disappearance in the gastric compartment and the persistence in the intestinal compartment suggest that these polypeptides are sensitive to pepsin and resist the action of pancreatin. The rest of the bands present in the intestinal

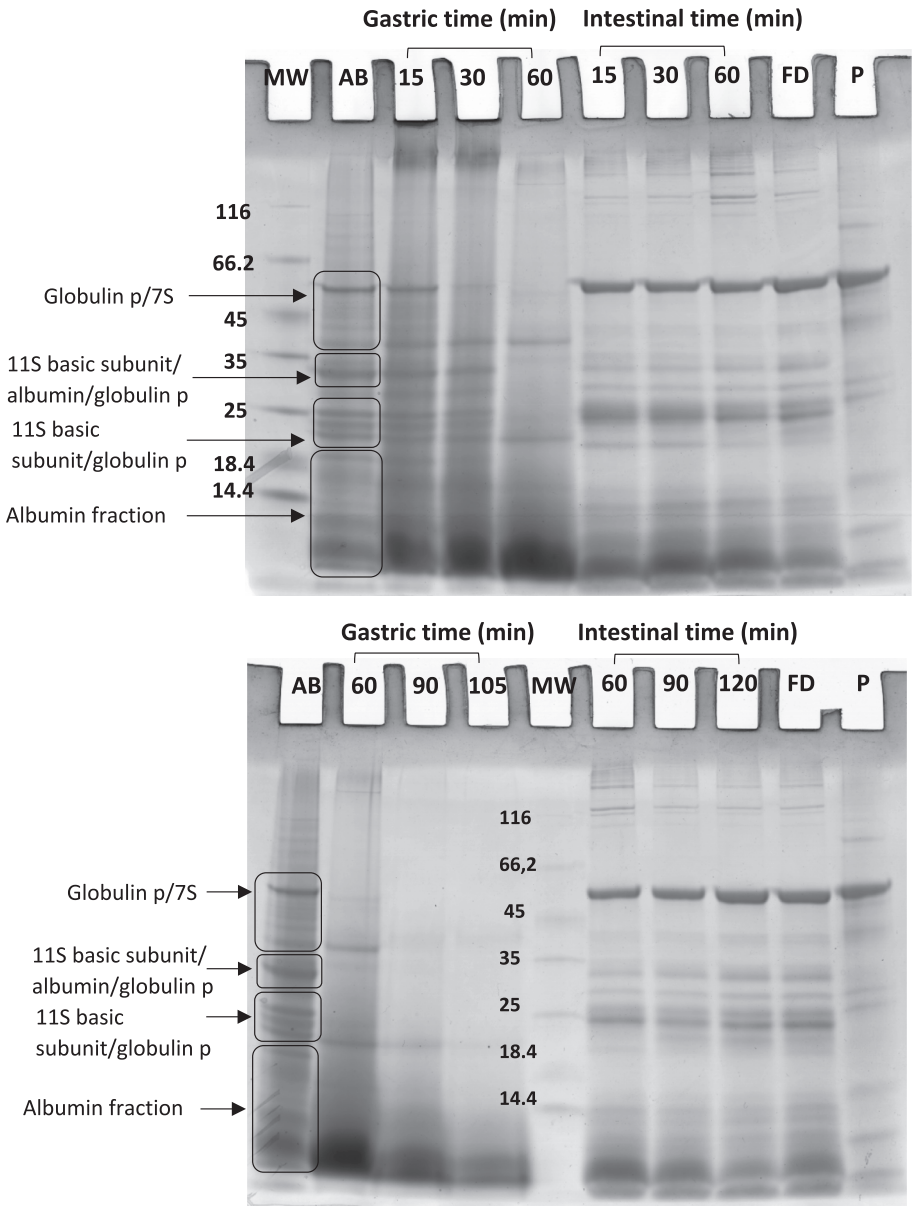

Fig. 3. SDS-PAGE gradients gels 8–16% in reducing conditions of the gastric and intestinal phases of dynamic *in vitro* digestion with time-resolved sampling. Molecular weight (MW), Amaranth beverage (AB), Final digesta (FD) and Pancreatin (P).

profiles correspond to the pancreatin used in the assays. Taken together, the results shown suggest that the most resistant polypeptides to digestion were 11S basic subunit (31.9 KDa) and P globulin (25 KDa); it cannot be ruled out these polypeptides could be hydrolyzed by brush border enzymes in intestinal cells.

3.3. Particle size distribution

Particle size distribution was determined during gastric phase (Fig. 4). The average particle size of AB was significantly influenced by gastric phase and digestion time. Initial particle size ($D_{4,3}$) of AB was 104 ± 21 μm with a slight increase in presence of SDS (125 ± 16 μm) as shown in Fig. 4 **panel A,** without significance difference ($p < 0.05$). Monomodal behavior was observed in both distributions. Manassero et al. (2020) analyzed the particle size of different amaranth beverages and found modes in volume distribution of 0.9, 19.9 and 239.5 μm in a liquid sample with the same composition as used in this work. According to these authors thermal treatment and gum addition promoted the formation of larger aggregates. Furthermore, it should be added the freeze-dried step carried out for this study and the consequent solubilization, probably contributing to the formation of new aggregates. The bigger particles found in AB before digestion (104.4 μm, 0 min) also suggest an incomplete solubilization of amaranth proteins. As it was mentioned before, protein aggregation during technological processes could occur or also the incomplete solubilization of proteins cannot be counteracted by the presence of SDS. So, non-soluble and soluble aggregates were presented in the beginning of gastric phase. Despite the presence of aggregates since early stages of gastric digestion, it should be mentioned that gastric emptying was not compromised. As gastric digestion phase progressed, De Broucker diameter increase from 104 μm to a value of 176 ± 34 μm, 222 ± 16 μm, 256 ± 42 μm, 330 ± 138 μm, and 320 ± 133 μm in 15, 30, 60, 90 and 105 min respectively (Fig. 4; **panel b, c, d, e, f**). Significant differences were found between time 0 and times 60 ($p < 0.05$), 90 ($p < 0.05$) and 105 min ($p < 0.05$). Distributions shapes slightly change until reaching 90 min where a shoulder was observed in the left part of the curve with similar behavior at 105 min. In presence of SDS, particle size significantly decreased from 125 μm ($t = 0$) to 94 ± 5 μm ($p > 0.001$), 84 ± 12 μm ($p = 0.0001$), 51 ± 8

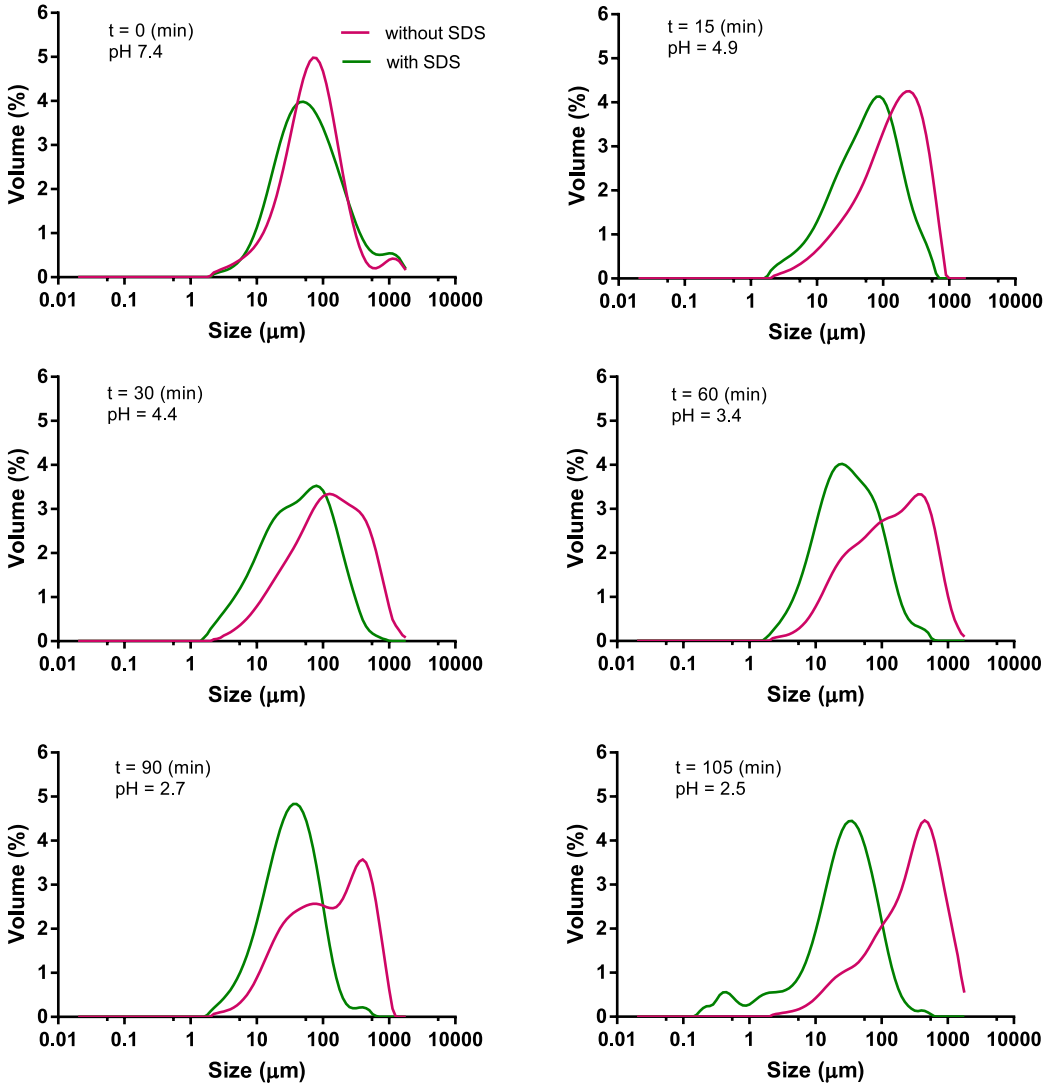

Fig. 4. Particle size distribution of amaranth-based beverage during gastric phase during different sampling times (t = 0, 15, 30, 60, 90 and 105 min). Pink line means without SDS addition and green line in presence of SDS.

µm ($p < 0.0001$), 50 ± 2 µm ($p < 0.0001$) and 45 ± 3 µm ($p < 0.0001$) in 15, 30, 60, 90 and 105 min respectively. To compare diameter values in presence and absence of SDS, an aggregation index was calculated. During gastric phase, aggregation index was increased from 45.8 % to 61.6 %, 79.6 %, 83.8 %, and 84.5 % in 15, 30, 60, 90 and 105 min respectively. Clearly, these values indicate a strong aggregation process led by amaranth soluble proteins.

While gastric digestion step progressed, fluid composition and pH changed. Proteins present in AB not only change size due to proteolysis as gel electrophoresis and degree of hydrolysis showed (Figs. 2 and 3), but also changed the net charge that evidently, influence protein interactions to form aggregates (Fig. 1**a**). At this point, interactions between lipids and proteins might also be involved even though in much less extent because lipid content was less than 1 % in initial AB. While gastric digestion progressed, during the first 60 min (aggregation index 79.6 %), amaranth proteins seem to evidence most of the aggregation. During this time the pH decreased from 7.4 in AB before digestion to a value of 3.4 (60 min) (Fig. 1**a**). Larger particles aggregates were formed when pH was close to the isoelectric point of amaranth proteins (Konishi et al., 1985; Marcone & Yada, 1992; Segura-Nieto et al., 1992). Under these conditions protein–protein interactions are favored, electrostatic repulsion decrease, and hydrophobic residues are exposed due to protein denaturation (Malaki Nik et al., 2011; Wang et al., 2021). Acidic pH may contribute to protein–protein interactions and consequently the formation of aggregates, similar behavior was found by Wang et al. (2020) using an almond milk subjected to gastric digestion. Acidification played a key role in the formation of larger aggregates particles in faba bean and pea infant formulas, FIF and PIF respectively, during the first 60 min of gastric digestion. Almost all smallest particles disappeared in this time when pH was 5.89 (Le Roux et al., 2020). These authors reported modal diameters of 0.8 and 10.0 µm for FIF, and 0.8 and 56.4 µm for PIF, before digestion. Moreover, distribution was bimodal. After 60 min of gastric digestion, modal diameters changed to a value of 31.7 µm and 12.6 µm for PIF and FIF, respectively. These values correspond to protein and lipid aggregates and were noticeably smaller than particle sizes found for amaranth proteins. Despite samples (AB, PIF and FIF) showed increase in particle size and formation of aggregates while gastric digestion goes on, evidently, the initial non-soluble aggregates in AB played an outstanding role in particle size.

3.4. ACE inhibitory capacity and peptide identification

The inhibitory activity on ACE after gastric digestion, final digesta and fractionated fraction of the final digesta were evaluated. Fig. 5 shows the ACE inhibitory activity against protein concentration of the samples. The digest obtained after 105 min of gastric digestion showed a

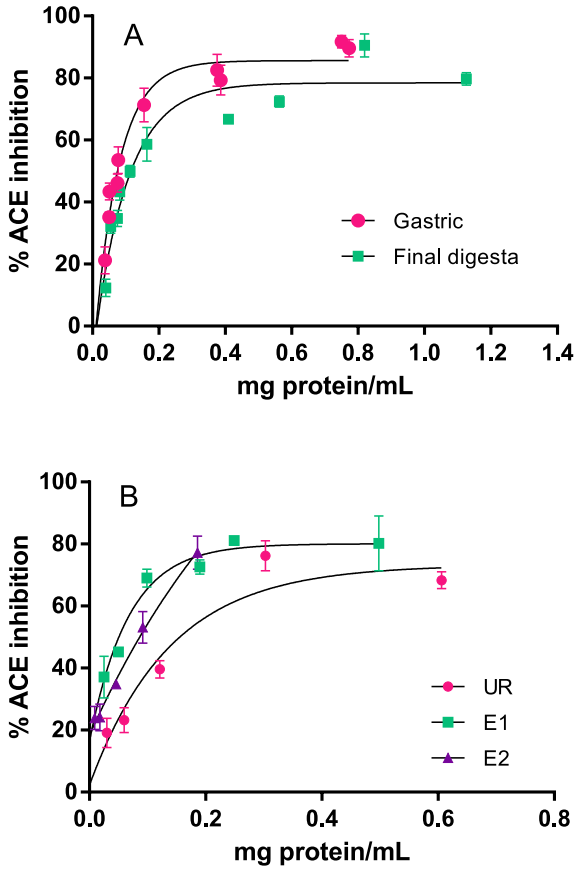

Fig. 5. Angiotensin converting enzyme (ACE) inhibition curves using gastric (105 min) and final digesta in panel A. Panel B shows unretained fraction (UR), eluted 1 (E1) and eluted 2 (E2) fractions obtained from final digesta. Protein/peptides content was measured by BCA method.

high ACE inhibition capacity (approx. 90 % inhibition, $IC_{50} = 80 \pm 10$ μg protein/mL), greater than that presented by the final digesta (approx. 85 % inhibition, $IC_{50} = 140 \pm 20$ μg/mL) (Fig. 5**a**). These results would indicate that AB is a potential source of antihypertensive peptides after digestion and suggest that active peptides released in the gastric compartment are hydrolyzed in the intestinal compartment and/or that new active peptides are released, but less potent than those found in the gastric compartment. Similar results were found by Vilcacundo et al. (2019) in the kiwicha (*Amaranthus caudatus*) protein concentrate where IC_{50} after gastric digestion was 39.0 ± 3.0 μg peptide/mL and, in the final stage of intestinal digestion was 88.0 ± 14.0 μg peptide/mL. Authors indicated that some ACE-inhibitory peptides released by pepsin were degraded by pancreatin.

To obtain purer fractions and eventually identify the main peptides present, the final digesta was subjected a fractionation step in C18 Sep-pack cartridges and three fractions were obtained and analyzed by RP-HPLC. Fractions were called unretained (UR), eluted 1 (E1) and eluted 2 (E2) as it was explained in section 2.7. The ACE inhibitory activity of the three selected fractions was then determined (Fig. 5**b**). The results showed that the purified fractions (E1 and E2) presented a greater inhibitory activity of ACE than the final digest, being the IC_{50} values 210 ± 40 μg/mL, 50 ± 10 μg/mL, and 60 ± 10 μg /mL for UR, E1, and E2 fraction, respectively. Fraction E2 was chosen for peptide identification based on the lowest IC_{50} and purity according to RP-HPLC chromatogram. Fraction E2 was analyzed by NanoLC-ESI-MS/MS before concentration. For the identification of peptides from this fraction, ASM2621246v1 of amaranthus tricolor was used as a reference genome. This genome was selected as it is the newest and most complete of the 8 amaranth genomes included in the National Center for Biotechnology Information (https://www.ncbi.nlm.nih.gov, NCBI RefSeq assembly GCF_026212465.1). A total of 26 peptide sequences were identified (Table 3). Three of them, AGLPVIM, ILVDGNDPR, SADKILDPL correspond to *A. hypochondriacus* agglutinin. Of the three peptide sequences identified as 11S in *A. tricolor*, only one of them, IERGEGIMGV, has an E value according to the alignment carried out with BLAST (https://blast.ncbi.nlm.nih.gov/Blast.cgi) of 0.61, which indicates homology between this sequence from *A. tricolor* and the one encrypted in *A. hypochondriacus*. Two other sequences assigned to the cocosin protein of *A. tricolor*, FDDMVQEGQLLVVPQ and LVFDDMVQEGQ, are also found in 11S of *A. hypochondriacus* with E values of 0.003 and 4.5, respectively, values that ensure homology between both sequences/proteins and are within the accepted ranges of biological variability. The rest of the identified sequences correspond to two metabolic proteins of *A. tricolor*, cocosin 1-like and NADPH-dependent aldehyde reductase 1.

It is worth asking why so few peptide sequences from the major storage proteins of the grain, 11S and 7S, has been detected. Most likely, the rest of the grain proteins are more resistant to hydrolysis than 11S and 7S, which, as we have shown, are digested both at the gastric and intestinal level (Fig. 3). Ayala-Niño et al. (2020) obtained similar results. They identified peptides with high antihypertensive, antithrombotic and antioxidant activity from two RP-HPLC fractions of an amaranth protein isolate hydrolyzed with alcalase and flavourzyme. Of the 21 peptides identified, 6 came from agglutinin and the rest from granule-bound starch synthase I. None of them came from the 11S and 7S globulin fractions. On the other hand, it should be remembered that in the analysis carried out, peptides with a number of amino acids less than 6 cannot be identified. Recently, in a multi-centre peptidomics research of food digesta (Portman et al 2023), the limitations of using MS-technologies in identifying peptides only in the range of 500–3500 Da and the loss of information related to small peptides are highlighted. On the other hand, the need to have protocols to analyze harmonized digesta is also emphasized since the results obtained are dependent on the equipment and conditions used in each laboratory. The detected peptides contain short sequences previously associated with ACE inhibition from 11S and metabolic proteins of *Amaranthus hypochondriacus*, (Montoya-Rodríguez et al., 2014 and 2015, Ayala-Niño et al., 2019, Sánchez-López et al., 2021). In addition, several of the identified sequences contain V, A and hydrophobic amino acids at the C-terminal end such as P, L and M and aliphatic amino acids at the N-terminal end, which have been associated with sequences of ACE inhibitors (Hanafi et al., 2018; Zhang-Ji et al., 2018, Ayala-Niño et al., 2019). 7S Globulin also shows potential peptide sequence with ACE inhibitory activity: PR, PL, GG, GF (Quiroga et al., 2012).

According to the analysis carried out with BIOPEP-UWM online tool (https://biochemia.uwm.edu.pl/) the detected sequences contain the following di- or tripeptides associated with ACE inhibitors: **AGLP**VIM: GLP, GL, AG and LP; **IL**VDGND**PR**: PR, GD and IL; SADK**ILDPL**: PL and IL; **IERGEGIMGV**: GI, GV, MG, IE, EG, RG and ER and **LVF**DDMVQ**EGQ**: VF, GQ, EG, LVF. Considering these results, the sequence most likely to inhibit ACE would be **IERGEGIMGV**.

Particularly striking are the sequences ILVDGNDPR and SADKILDPL, which with small differences has been previously detected in digesta of amaranth protein isolates obtained by gastrointestinal digestion process using a static method (LVDGNDPR and SADKILDPL, Sabbione et al., 2016) and in 11S globulin samples fermented with *Lactobacillus plantarum* (LVDGNDPRE, Sanchéz-López et al., 2021). In all these cases, grains of *Amaranthus hypochondriacus* were used. Sabbione et al. (2016) associated these sequences with a potential capacity to inhibit thrombin and Sánchez-López et al. (2021) with the inhibition of DPP4.

The results obtained suggest that some of the peptide sequences identified may be responsible for the ACE inhibition activity detected by *in vitro* assays. It cannot be ruled out that peptide sequences with a length of less than five amino acids exist in the digesta, which may be inhibitors of the ACE enzyme and have not been detected by the protocol used to detect the peptide sequences. For this reason, *in silico* assays are

Table 3
Potentially bioactive peptide sequences identified.

Sequence	Protein source	Species	Accession number
AGLPVIM	Agglutinin	Amaranthus hypochondriacus	tr|Q38719|Q38719_AMAHP
ILVDGNDPR			
SADKILDPL			
IERGEGIMGV	11S globulin	Amaranthus tricolor	XP_057517640.1
		Amaranthus hypochondriacus	CAA57633.1
		Amaranthus hypochondriacus	3QAC_A
		Amaranthus hypochondriacus	ABM66807.1
AIPPGAVH	11S globulin	Amaranthus tricolor	XP_057517640.1
TLPNFFPFPR			
FDDMVQEGQLLVVPQ	Cocosin 1-like	Amaranthus tricolor	XP_057531257.1
		Amaranthus hypochondriacus	CAA57633.1
		Amaranthus hypochondriacus	3QAC_A
		Amaranthus hypochondriacus	ABM66807.1
LVFDDMVQEGQ	Cocosin 1-like	Amaranthus tricolor	XP_057531257.1
		Amaranthus hypochondriacus	CAA57633.1
		Amaranthus hypochondriacus	3QAC_A
		Amaranthus hypochondriacus	ABM66807.1
GLLIPEWDREES	Cocosin 1-like	Amaranthus tricolor	XP_057531257.1
HGSEWDPR			
LLIPEWDREES			
LVFDDM			
NPPFLPA			
NPPFLPAG			
PAHGSEWDPR			
PGHGSQRPT			
PTHGSEWDPR			
RVEGDLGLLIPE			
SFNPPFLPA			
SFNPPFLPAG			
VEGDLGLLIPE			
YPGHGSQRPA			
YPGHGSQRPT			
SFGSQVPM	NADPH	Amaranthus tricolor	XP_057549860.1
VNGVAPGPIWTP	aldehydereductase 1		
VNGVAPGPIWTPL			

being carried out in the laboratory that will provide more data on the potential mechanism of interaction of the identified sequences with the ACE enzyme. According to the results achieved in these studies, the potentially most active peptides will be synthesized to subsequently validate their ACE inhibition action *in vitro*.

4. Conclusions

Plant protein-based beverages are increasingly appreciated by consumers. The results obtained in this work show that the proteins present in a beverage formulated with amaranth grains, after being subjected to a simulated gastrointestinal digestion process, are an efficient source of peptides with antihypertensive capacity. During the gastric digestion aggregation and denaturation of amaranth protein was observed, mainly due to the variation in pH, which induces variations in their net charge. At the same time, they are partially hydrolyzed by pepsin, being 20.9 kDa and 40.1 kDa polypeptides the most resistant. Despite the presence of aggregates since early stages of gastric digestion, gastric emptying was not compromised. Further experiments are needed to elucidate the kinetics of amaranth protein interactions and the effect of the small amount of gums added to the beverage during gastric digestion. During the intestinal phase both the aggregates and the individual polypeptide species are sensitive to the action of pancreatin, except for 31.9 KDa and 25 KDa bands corresponding to basic subunit 11S and globulin P.

The final digesta obtained, as well as fractions obtained from them, showed a remarkable antihypertensive activity with IC_{50} values that varied between 140 μg/mL, up to 50 μg/mL, in the most active fraction obtained from the digesta. From fraction E2, 6 peptide sequences were identified, which contain internal sequences previously identified as antihypertensive, particularly IERGEGIMGV. This is the first time, to our knowledge, that the presence of bioactive peptides has been shown in digesta obtained with the dynamic system of a vegetable beverage, which is highly promising for the formulation of functional foods based on amaranth proteins.

CRediT authorship contribution statement

Santiago E. Suárez: Writing – review & editing, Writing – original draft, Investigation, Formal analysis, Conceptualization. **Hanitra Rabesona:** Writing – review & editing, Investigation, Formal analysis. **Olivia Ménard:** Writing – review & editing, Resources, Investigation, Formal analysis. **Julien Jardin:** Writing – review & editing, Investigation, Formal analysis. **Marc Anton:** Writing – review & editing, Supervision, Resources, Formal analysis. **María Cristina Añón:** Writing – review & editing, Writing – original draft, Supervision, Resources, Project administration, Funding acquisition, Conceptualization.

Declaration of competing interest

The authors declare that they have no known competing financial interests or personal relationships that could have appeared to influence the work reported in this paper.

Data availability

Data will be made available on request.

References

Añón, M.C., Quiroga, A.V., Scilingo, A.A., Tironi, V.A., Sabbione, A.C., Nardo, A.E., Suárez, S.E., García Fillería, S.F. (2021). Action of amaranth peptides on the cardiovascular system. In B. S. R. Repo-Carrasco-Valencia, M. C. Tomas (Eds). *Native crops in Latin America: Processing and nutraceutical aspects.* (pp. 209-236). Editorial CRC Press, Taylor and Francis Group. ISBN 978-0-367-53140-9.

Ayala-Niño, A., Rodríguez-Serrano, G. M., González-Olivares, L. G., Contreras-López, E., Regal-López, P., & Cepeda-Saez, A. (2019). Sequence identification of bioactive peptides from amaranth seed proteins (Amaranthus hypochondriacus spp.). *Molecules, 24*(17), 3033. https://doi.org/10.3390/molecules24173033

Ayala-Niño, A., Castañeda-Ovando, A., Jaimez-Ordaza, J., Rodrıguez-Serrano, G. M., Sanchez-Franco, J. A., & Gonzalez-Olivare, L. G. (2020). Novel bioactive peptides sequences released by in vitro digestion of proteins isolated from Amaranthus hypochondriacus. *Natural Product Research, 36*(13), 3485–3488. https://doi.org/10.1080/14786419.2020.1862837

Bertrand-Harb, C., Nicolas, M. G., Dalgalarrondo, M., & Chobert, J. M. (1993). Determination of alkylation degree by three colorimetric methods and amino acid analysis: A comparative study. *Sciences Des Aliments, 13*(3), 577–584.

Craig, W. J., & Fresán, U. (2021). International analysis of the nutritional content and a review of health benefits of non-dairy plant-based beverages. *Nutrients, 13*(3), 1–14. https://doi.org/10.3390/nu13030842

Cushman, D. W., & Cheung, H. S. (1971). Spectophotometric assay and properties of the angiotensin I-converting enzyme of rabbit lung. *Biochemical Pharmacology, 20*, 1637–1648. https://doi.org/10.1016/0006-2952(71)90292-9

Deglaire, A., Oliveira, S. D., Jardin, J., Briard-Bion, V., Kroell, F., Emily, M., Menard, O., Bourlieu, C., & Dupont, D. (2019). Impact of human milk pasteurization on the kinetics of peptide release during in vitro dynamic digestion at the preterm newborn stage. *Food Chemistry, 281*, 294–303. https://doi.org/10.1016/j.foodchem.2018.12.086

Dupont, D., Alric, M., Blanquet-Diot, S., Bornhorst, G., Cueva, C., Deglaire, A., Denis, S., Ferrua, M., Havenaar, R., Lelieveld, J., Mackie, A. R., Marzorati, M., Menard, O., Minekus, M., Miralles, B., Recio, I., & Van den Abbeele, P. (2019). Can dynamic in vitro digestion systems mimic the physiological reality? *Critical Reviews in Food Science and Nutrition, 59*(10), 1546–1562. https://doi.org/10.1080/10408398.2017.1421900

Egger, L., Ménard, O., Baumann, C., Duerr, D., Schlegel, P., Stoll, P., Vergères, G., Dupont, D., & Portmann, R. (2019). Digestion of milk proteins: Comparing static and dynamic in vitro digestion systems with in vivo data. *Food Research International, 118*, 32–39. https://doi.org/10.1016/j.foodres.2017.12.049

Fritz, M., Vecchi, B., Rinaldi, G., & Añón, M. C. (2011). Amaranth seed protein hydrolysates have in vivo and in vitro antihypertensive activity. *Food Chemistry, 126*(3), 878–884. https://doi.org/10.1016/j.foodchem.2010.11.065

Hanafi, M. A., Hashim, S. N., Chay, S. Y., Ebrahimpour, A., Zarei, M., Muhammad, K., & Saari, N. (2018). High angiotensin-I converting enzyme (ACE) inhibitory activity of Alcalase-digested green soybean (Glycine max) hydrolysates. *Food Research International, 106*, 589–597. https://doi.org/10.1016/j.foodres.2018.01.030

Jiménez-Munoz, L., Brodkorb, A., Gómez-Mascaraque, L. G., & Corredig, M. (2021). Effect of heat treatment on the digestion behavior of pea and rice protein dispersions and their blends, studied using the semi-dynamic INFOGEST digestion method. *Food and Function, 12*(18), 8747–8759. https://doi.org/10.1039/d1fo01223a

Konishi, Y., Horikawa, K., Oku, Y., Azumaya, J., & Nakatani, N. (1991). Extraction of two albumin fractions from amaranth grains: Comparison of some physicochemical properties and the putative localization in the grains. *Agricultural and Biological Chemistry, 55*(11), 2745–2750. https://doi.org/10.1080/00021369.1991.10857150

Konishi, O., Fumita, Y., Ikeda, K., & Fuwa, H. (1985). Isolation and characterization of globulin from seeds of amaranthus hypochondriacus L. *Agricultural and Biological Chemistry, 49*(5), 1453–1459. https://doi.org/10.1271/bbb1961.49.1453

Laemmli, U. K. (1970). Cleavage of structural proteins during the assembly of the head of bacteriophage T4. *Nature, 227*, 680–684.

Langella, O., Valot, B., Balliau, T., Blein-Nicolas, M., Bonhomme, L., & Zivy, M. (2017). X!TandemPipeline: A tool to manage sequence redundancy for protein inference and phosphosite identification. *Journal of Proteome Research, 16*(2), 494–503. https://doi.org/10.1021/acs.jproteome.6b00632

Lawrence, A. M., & Besir, H. (2009). Staining of proteins in gels with Coomassie G-250 without organic solvent and acetic acid. *Journal of Visualized Experiments, 30*, 2–4. https://doi.org/10.3791/1350

Le Roux, L., Ménard, O., Chacon, R., Dupont, D., Jeantet, R., Deglaire, A., & Nau, F. (2020). Are faba bean and pea proteins potential whey protein substitutes in infant formulas? An in vitro dynamic digestion approach. *Foods, 9*(3). https://doi.org/10.3390/foods9030362

Malaki Nik, A., Wright, A. J., & Corredig, M. (2011). Impact of interfacial composition on emulsion digestion and rate of lipid hydrolysis using different in vitro digestion models. *Colloids and Surfaces B: Biointerfaces, 83*(2), 321–330. https://doi.org/10.1016/j.colsurfb.2010.12.001

Manassero, C. A., Añón, M. C., & Speroni, F. (2020). Development of a high protein beverage based on amaranth. *Plant Foods for Human Nutrition, 75*(4), 599–607. https://doi.org/10.1007/s11130-020-00853-9

Marcone, M. F., & Yada, R. Y. (1992). Study of the charge profile and covalent subunit association of the oligomeric seed globulin from amaranthus hypochondriacus. *Journal of Agricultural and Food Chemistry, 40*(3), 385–389. https://doi.org/10.1021/jf00015a005

Martínez, E. N., & Añón, M. C. (1996). Composition and structural characterization of amaranth protein isolates. an electrophoretic and calorimetric study. *Journal of Agricultural and Food Chemistry, 44*(9), 2523–2530. https://doi.org/10.1021/jf960169p

Martínez, E. N., Castellani, O. F., & Añón, M. C. (1997). Common molecular features among amaranth storage proteins. *Scanning, 3832–3839*. https://doi.org/10.1021/JF9700384

Ménard, O., Cattenoz, T., Guillemin, H., Souchon, I., Deglaire, A., Dupont, D., & Picque, D. (2014). Validation of a new in vitro dynamic system to simulate infant digestion. *Food Chemistry, 145*, 1039–1045. https://doi.org/10.1016/j.foodchem.2013.09.036

Ménard, O., Picque, D., & Dupont, D. (2015). The DIDGI® System. In B. K. Verhoeckx, P. Cotter, I. López-Expósito, C. Kleiveland, T. Lea, A. Mackie, T. Requena, D. Swiatecka, & H. Wichers (Eds.), *The impact of food bioactives on health, in vitro and ex vivo models* (pp. 73–81). Publisher Springer Cham. ISBN 978-3-319-16104-4.

Mennah-Govela, Y. A., Singh, R. P., & Bornhorst, G. M. (2019). Buffering capacity of protein-based model food systems in the context of gastric digestion. *Food and Function, 10*(9), 6074–6087. https://doi.org/10.1039/c9fo01160a

Minekus, M., Marteau, P., Havenaar, R., & Huis in T Veld, J. H. J.. (1995). A multicompartmental dynamic computer-controlled model simulating the stomach and small intestine. *Alternatives to Laboratory Animals, 23*, 197–209. https://doi.org/10.1177/026119299502300205

Montoya-Rodríguez, A., de Mejía, E. G., Dia, V. P., Reyes-Moreno, C., & Milán-Carrillo, J. (2014). Extrusion improved the anti-inflammatory effect of amaranth (Amaranthus hypochondriacus) hydrolysates in LPS-induced human THP-1 macrophage-like and mouse RAW 264.7 macrophages by preventing activation of NF-κB signaling. *Molecular Nutrition and Food Research, 58*(5), 1028–1041. https://doi.org/10.1002/mnfr.201300764

Montoya-Rodríguez, A., Gómez-Favela, M. A., Reyes-Moreno, C., Milán-Carrillo, J., & González de Mejía, E. (2015). Identification of bioactive peptide sequences from amaranth (Amaranthus hypochondriacus) seed proteins and their potential role in the prevention of chronic diseases. *Comprehensive Reviews in Food Science and Food Safety, 14*(2), 139–158. https://doi.org/10.1111/1541-4337.12125

Munekata, P. E. S., Domínguez, R., Budaraju, S., Roselló-Soto, E., Barba, F. J., Mallikarjunan, K., Roohinejad, S., & Lorenzo, J. M. (2020). Effect of innovative food processing technologies on the physicochemical and nutritional properties and quality of non-dairy plant-based beverages. *Foods, 9*(3), 1–16. https://doi.org/10.3390/foods9030288

Nardo, A. E., Suárez, S., Quiroga, A. V., & Añón, M. C. (2020). Amaranth as a source of antihypertensive peptides. *Frontiers in Plant Science, 11*(September), 1–15. https://doi.org/10.3389/fpls.2020.578631

Portmann, R., Jiménez-Barrios, P., Jardin, J., Abbühl, L., Barile, D., Danielsen, M., Huang, Y. P., Dalsgaard, T. K., Miralles, B., Briard-Bion, V., Cattaneo, S., Chambon, C., Cudennec, B., De Noni, I., Deracinois, B., Dupont, D., Duval, A., Flahaut, C., López-Nicolás, R., Nehir El, S., Pica, V., Santé-Lhoutellier, V., Stuknyté, M., Theron, L., Sayd, T., & Recio., I., Egger, L.. (2023). A multi-centre peptidomics investigation of food digesta: Current state of the art in mass spectrometry analysis and data visualisation. *Food Research International, 169*(April). https://doi.org/10.1016/j.foodres.2023.112887

Quiroga, A., Martínez, E. N., Rogniaux, H., Geairon, A., & Añón, M. C. (2010). Amaranth (Amaranthus hypochondriacus) vicilin subunit structure. *Journal of Agricultural and Food Chemistry, 58*(24), 12957–12963. https://doi.org/10.1021/jf103296n

Quiroga, A. V., Aphalo, P., Nardo, A. E., & Añón, M. C. (2017). In vitro modulation of renin-angiotensin system enzymes by amaranth (amaranthus hypochondriacus) protein-derived peptides: alternative mechanisms different from ACE inhibition. *Journal of Agricultural and Food Chemistry, 65*(34), 7415–7423. https://doi.org/10.1021/acs.jafc.7b02240

Quiroga, A. V., Aphalo, P., Ventureira, J. L., Martínez, E. N., & Añón, M. C. (2012). Physicochemical, functional and angiotensin converting enzyme inhibitory properties of Amaranth (Amaranthus hypochondriacus) 7S globulin. *Journal of the Science of Food and Agriculture, 92*(2), 397–403. https://doi.org/10.1002/jsfa.4590

Quirós, A., Hernández-Ledesma, B., Ramos, M., Amigo, L., & Recio, I. (2005). Angiotensin-converting enzyme inhibitory activity of peptides derived from caprine kefir. *Journal of Dairy Science, 88*(10), 3480–3487. https://doi.org/10.3168/jds.S0022-0302(05)73032-0

Rodríguez, M., García Fillería, S., & Tironi, V. (2020). Simulated gastrointestinal digestion of amaranth flour and protein isolate: Comparison of methodologies and release of antioxidant peptides. *Food Research International, 138A*, 109735. https://doi.org/10.1016/j.foodres.2020.109735

Rodríguez, M., & Tironi, V. (2023). Chemical and cell antioxidant activity of amaranth flour and beverage after simulated gastrointestinal digestion. *Role of peptides. Food Research International, 173*, Article 113410. https://doi.org/10.1016/j.foodres.2023.113410

Sabbione, A. C., Nardo, A. E., Añón, M. C., & Scilingo, A. (2016). Amaranth peptides with antithrombotic activity released by simulated gastrointestinal digestion. *Journal of Functional Foods, 20*(6), 204–214. https://doi.org/10.1016/j.jff.2015.10.015

Sánchez-López, F., Robles-Olvera, V. J., Hidalgo-Morales, M., & Tsopmo, A. (2021). Angiotensin-I converting enzyme inhibitory activity of Amaranthus hypochondriacus seed protein hydrolysates produced with lactic bacteria and their peptidomic profiles. *Food Chemistry, 363*, Article 130320. https://doi.org/10.1016/j.foodchem.2021.130320

Segura-Nieto, M., Vázquez-Sánchez, N., Rubio-Velázquez, H., Olguin-Martínez, L. E., Rodríguez-Nester, C. E., & Herrera-Estrella, L. (1992). Characterization of amaranth (Amaranthus hypochondriacus L.) seed proteins. *Journal of Agricultural and Food Chemistry, 40*(9), 1553–1558. https://doi.org/10.1021/jf00021a016

Suárez, S., Aphalo, P., Rinaldi, G., Añón, M. C., & Quiroga, A. (2020). Effect of amaranth proteins on the RAS system. In vitro, in vivo and ex vivo assays. *Food Chemistry, 308*. https://doi.org/10.1016/j.foodchem.2019.125601

Suarez, S. E., & Añón, M. C. (2017). Comparative behaviour of solutions and dispersions of amaranth proteins on their emulsifying properties. *Food Hydrocolloids Suarez Food Hydrocolloids*. https://doi.org/10.1016/j.foodhyd.2017.07.042

Velarde-Salcedo, A. J., Bojórquez-Velázquez, E., & de Barba de la Rosa, B.. (2019). Amaranth. In B. S. J. Johnson, & T. Wallace (Eds.), *Whole grains and their bioactives: composition and helth* (pp. 209–250). John Wiley & Sons Ltd.

Vilcacundo, R., Martínez-Villaluenga, C., Miralles, B., & Hernández-Ledesma, B. (2019). Release of multifunctional peptides from kiwicha (Amaranthus caudatus) protein

under in vitro gastrointestinal digestion. *Journal of the Science of Food and Agriculture, 99*(3), 1225–1232. https://doi.org/10.1002/jsfa.9294

Wang, X., Ye, A., Dave, A., & Singh, H. (2021). In vitro digestion of soymilk using a human gastric simulator: Impact of structural changes on kinetics of release of proteins and lipids. *Food Hydrocolloids*, *111*(July 2020), 106235. Doi: 10.1016/j.foodhyd.2020.106235.

Wang, X., Ye, A., & Singh, H. (2020). Structural and physicochemical changes in almond milk during: In vitro gastric digestion: Impact on the delivery of protein and lipids. *Food and Function, 11*(5), 4314–4326. https://doi.org/10.1039/c9fo02465d

Wegrzyn, T. F., Acevedo-Fani, A., Loveday, S. M., & Singh, H. (2021). In vitro dynamic gastric digestion of soya protein/milk protein blended beverages: Influence of protein composition and co-processing. *Food and Function, 12*(6), 2605–2616. https://doi.org/10.1039/d0fo02742a

Zhang-Ji, Q., Yuang-Yuang, Z., Gun-Woo, O., Seong-Yeong, H., Won-Sun, P., & Il-Whan, C. (2018). Antioxidant and angiotensin I converting enzyme inhibition effects and antihypertensive effect in spontaneously hyertenisve rats of peptide isolated from boiled abalone by-products, Hallotis discus hannai. *Journal of Aquatic Food Product Technology, 27*(9), 946–996. https://doi.org/10.1080/10498850.2018.1518361